Food and Chemical Toxicology 133 (2019) 110796

Contents lists available at ScienceDirect

Food and Chemical Toxicology

journal homepage: www.elsevier.com/locate/foodchemtox

Red raspberry extract (*Rubus idaeus* L *shrub*) intake ameliorates hyperlipidemia in HFD-induced mice through PPAR signaling pathway

Lijun Tu[a], Hanju Sun[a,b,*], Mingming Tang[a], Jinlong Zhao[a], Zuoyong Zhang[a], Xianbao Sun[a], Shudong He[a,b,**]

[a] School of Food and Biological Engineering, Engineering Research Center of Bio-process of Ministry of Education, Hefei University of Technology, Hefei, 230009, PR China
[b] Anhui Province Key Laboratory of Functional Compound Seasoning, Anhui Qiangwang Seasoning Food Co., Ltd., Jieshou, 236500, Anhui, PR China

ARTICLE INFO

Keywords:
Red raspberry
High-fat diet
Hyperlipidemia
Transcriptome analysis
Triglyceride
Cholesterol

ABSTRACT

Effects of red raspberry extract (RRE) intake on hyperlipidemia mice induced by high-fat diet (HFD) were investigated in this study. After intragastric gavage of RRE for 8 weeks, the body weight and the adipose tissue mass of mice in RRE administration groups significantly ($p < 0.05$) decreased compared to the group without RRE treatment. RRE treatment significantly ($p < 0.05$) lowered triglyceride and total cholesterol levels of hyperlipidemia mice. Pparα, Hmgcr, Ldlr, Cyp7a1, Acsl3, Pnpla2 and Pin4 were confirmed as the regulatory genes by transcriptome analysis and qRCR validation. According to KEGG pathway analysis, target genes such as Cyp7a1 and Pin4 were further regulated by the activation of PPARα resulting from RRE supplementation. Meanwhile, liver cholesterol synthesis and conversion were inhibited by the expressions of Hmgcr and Cyp7a1 genes regulated by RRE intake, and Ldlr gene was down-regulated to limit the transport of cholesterol. In addition, RRE treatment could accelerate the conversion from triglyceride to fatty acid. To conclusion, RRE intake would be a protection against diet-induced hypertriglyceridemia.

1. Introduction

Hyperlipidemia is a major risk factor that contributes to atherosclerosis and subsequent cardiovascular disease resulting in approximately 23.5% of all deaths in the world (Johnston et al., 2017). Long-time intake of high-fat diet could disorder lipid metabolism, usually characterized by higher total cholesterol (TC), triglyceride (TG) level and more fat accumulation which are the main characteristics of hyperlipidemia (Zhu et al., 2017). Furthermore, oxidation system disorders are usually accompanied by hyperlipidemia (Wang et al., 2017). The natural antioxidant system was destroyed due to increased reactive oxygen *in vivo*, which was as a consequence of long-term lipid metabolism disorder (Si et al., 2017). With the increasing attention to hyperlipidemia induced by high-fat diet, it is necessary to explore functional diet supplementation to prevent the progression of hyperlipidemia.

Compared with hyperlipidemia medicine, plant extracts have been considered to be more suitable for long-term diet supplementation because of the relatively low toxicity (Guo et al., 2011). It has been reported that the plant extracts rich in polyphenols and flavonoids had positive effect on lipid metabolism *in vivo* (Joseph et al., 2016; Lin et al., 2010). Crude ginger polyphenol extract inhibited the hypertrophy and hyperplasia of 3T3-L1 adipose cells (Park et al., 2012). Many berry extracts from such as cherry, chokeberry, bilberry and elderberry, were rich in anthocyanins and were associated with reducing hyperlipidemia and scavenging reactive oxygen species (Bell and Kristen, 2006; Seymour et al., 2008). Red raspberry is a kind of berry of *Rubus idaeus* L *shrub*, with an annual output of 400,000 tons per year in the world (Souza et al., 2014). However, there is a little attention to red raspberry products. Many literatures have reported raspberry intake showed a positive impact on human health because of its functional ingredients with flavonoids and polyphenols (Durgo et al., 2012; Noratto et al., 2017). Raspberry consumption has been proven to protect against diabetes-induced oxidative stress (Bibi et al., 2018). Meanwhile, raspberry was considered as a possible dietary supplementation for patients with ulcerative colitis and related gut inflammatory diseases (Bibi et al., 2018).

The purpose of this research was to assess the effects of red raspberry dietary supplementation on hyperlipidemia mice induced by HFD. In this study, red raspberry extract (RRE) was prepared and its

* Corresponding author. School of Food and Biological Engineering, Hefei University of Technology, Hefei, 230009, PR China.
** Corresponding author. School of Food and Biological Engineering, Hefei University of Technology, Hefei, 230009, PR China.
E-mail addresses: sunhanjv@163.com (H. Sun), shudong.he@hfut.edu.cn (S. He).

https://doi.org/10.1016/j.fct.2019.110796
Received 30 July 2019; Received in revised form 22 August 2019; Accepted 26 August 2019
Available online 28 August 2019

Abbreviations

LDLR	low density lipoprotein receptor
LC-TOF-MS/MS	liquid chromatography-time of fight mass spectrum
Mups	the major urinary proteins
Gapdh	glyceraldehyde-3-phosphate dehydrogenase
Hmox	heme oxygenase
ROS	reactive oxygen species
Pnpla2	patatin-like phospholipase domain containing 2
Vldlr	very-low-density lipoprotein receptor
Prkaa2	protein kinase, AMP-activated, alpha-2 catalytic subunit
Cdca7	cell division cycle-associated protein 7
Gtf2h5	general transcription factor IIH, polypeptide 5
Nfil3	nuclear factor, interleukin 3 regulated
Nrep	neuronal regeneration related protein
Ldlrap1	low density lipoprotein receptor adapter protein 1
Crp	C reactive protein
Nr0b2	nuclear receptor subfamily 0 group B member 2
Slc25a27	solute carrier family 25 (mitochondrial uncoupling protein), member 27

composition was identified by LC-TOF-MS/MS. Animal experiments were conducted to explore the inhibitory effect of the RRE on high-fat diet induced hyperlipidemia. The molecular mechanisms of RRE intake were analyzed by transcriptomics and were further confirmed by qPCR.

2. Materials and methods

2.1. Materials

Red raspberry were obtained from Daxinganling Chenglin Mountain Wild Treasure Co., Ltd. (Daxinganling, Heilongjiang Province, China). The raspberry were frozen and stored at −20 °C before analysis. X-5 resin was purchased from Samsung Resin Technology Co., Ltd. (AnHui Province, China). Ethanol, pectinase (50000 U/g) and other chemical reagents were purchased from Sinopharm Chemical Reagent Co., Ltd. (Shanghai, China). A pectinase enzyme activity unit (U) was defined as the amount of enzyme required to convert 1 μmol of pectin in 1 min.

2.2. Methods

2.2.1. Preparation of RRE

Red raspberry products were extracted according to the previous study (Abdel-Aal et al., 2018). The frozen fresh red raspberries were mixed with 15 vol of 1.0% (m/v) citric acid solution, and then crushed by a high speed grinder (HX-200, Xian Suqing Co., China). Subsequently, the pectinase was added to the red raspberry pulp (1 g/L). The mixing solutions were incubated at 40 °C for 2 h in dark bottles. At the end of the enzymatic hydrolysis, filtration was done by using ultrafiltration membrane (molecular weight cut-off: 8 kDa). The filtrate was then loaded on the X-5 resin column (3.5 × 50 cm) equilibrated with distilled water previously. Deionized water was used to elute the column to remove impurities (Abdel-Aal et al., 2018). Finally, the column was eluted by 80% ethanol solution (v/v) and the eluent was collected. RRE was dried by a freeze dryer and then stored at −80 °C. Freeze-dried RRE was used for animal experiments.

2.2.2. Liquid chromatography and mass spectrometric parameters

The freeze-dried RRE sample was dissolved with 1% aqueous formic acid and was filtered through a 0.22 μm filter. The RRE solution (4 μL) was injected into the HPLC system. LC-TOF-MS/MS detection was conducted by using X500R QTOF Mass Spectrometry System and Exion LC System (AB SCIEX Co., Ltd.) equipped with a T3 Column (Agilent Co., 2.1 × 150 mm, 2.5 μm). The following solvents constituted the mobile phase: 1% aqueous formic (A) acid and acetonitrile (B). The linear gradient was as follows: 0–6 min 2–95% B, 6–10 min 95% B, 10–11 min 95-2% B, 11–14 min 2% B. The flow rate was 0.3 mL/min and the column temperature was set at 40 °C. Curtain gas and ion source gas were set as 30 and 55 Psi, respectively. The ionspray voltage was set at 4500 V. The desolvation temperature was set at 550 °C. The data were collected and analyzed by OS1.5 workstation (AB SCIEX Co., Ltd.). The peak area ratio of the identified substance to the total area was regarded as the relative abundance of the substance.

2.2.3. Experimental animals and treatment

The experiment was carried out in accordance with the U.K. Animals (Scientific Procedures) Act. Six-week-old male mice (C57BL/6J) were purchased from Svens Laboratory Supplies Co., Ltd. (HeFei, China). All mice were housed in cages maintained at 25 ± 1 °C with 12 h of light/dark cycle and had ad libitum access to diet and water. After one week of adaptation, mice were randomly distributed into four dietary groups (n = 8 per each group). The normal diet received a standard commercial laboratory diet (315 kcalorie per 100 g feed) purchased from Nanjing Shengming Research Co., Ltd. The high-fat diet was composed of 55% normal diet, 10% egg yolk power, 20% lard, 6% soybean oil, 8% sugar and 1% cholesterol (409 calorie per 100 g feed). Mice in normal diet control group (NC) were fed with a normal diet. Mice in HFD control group (HC) was fed with a high-fat diet without RRE. The mice were fed with high fat diet and given a daily administration of 100, 200, 300 mg freeze-dried RRE per kilogram of body weight for 8 weeks, and were named HFD-low dose of RRE (HL), HFD-middle dose of RRE (HM) and HFD-high dose of RRE (HH), respectively. RRE treatment was conducted by intragastric administration of aqueous RRE solution and was separated from the diet. The body weight and food consumption were measured weekly. Energy intake was calculated as the product of food intake and energy ratio of food. At the end of the experiment, all mice were fasted for 12 h to eliminate the influence of foods such as exogenous cholesterol, and were then sacrificed by CO_2 asphyxiation for 2 min. The liver, perirenal and epididymal adipose tissues were weighed. The serum was immediately prepared from plasma and stored at −80 °C. The liver were immediately frozen and stored at −80 °C. The perirenal and epididymal adipose tissues were stored in fixative solution (Wuhan Sevier Biotechnology Co., Ltd.).

2.2.4. Biochemical analysis

The liver was homogenized in a saline (1:9, w/v) and the homogenate was centrifuged at 3000 rpm for 15 min. The upper aqueous phase was used to measure biochemical index. Serum samples were prepared by centrifugation at 3500 rpm for 10 min. Total bile acid, aspartate aminotransferase (AST), alanine aminotransferase (AST), total cholesterol (TC), triglyceride (TG), LDL cholesterol (LDL-C), and HDL-cholesterol (HDL-C), glutathione peroxidase (GSH-Px), catalase (CAT), superoxide dismutase (SOD), malondialdehyde (MDA) were measured by commercially kits purchased form Nanjing Jiancheng Bioengineering Institute (Nanjing, China).

2.2.5. Histological analysis

The epididymal adipose tissues were fixed in 10% buffered formalin for at least 24 h, then were embedded in paraffin and sectioned. The sections were then stained with hematoxylin and eosin (H&E) for adipocytes size analysis.

2.2.6. Transcriptome analysis

Total RNA in liver was extracted using commercial kit according to the guided procedure. Poly-Toligo-attached magnetic was used to purify Poly (A) RNA from total RNA. Subsequently, the mRNA was fragmented into small pieces using divalent cations. The cDNA library

was created by the reverse transcription of the cleaved RNA fragments. LluminaHiseq 4000 (LC Sciences, LLC., USA) was used to conduct the paired-end sequencing.

The reads were aligned to the UCSC (http://genome.ucsc.edu/) and mapped to the reference genome using HISAT package. StringTie was used to evaluate expression level by calculating FPKM and the genes expression were selected with statistical significance ($p < 0.05$) by R package. GOSeq R package was used to conduct Gene Ontology (GO) enrichment analysis. Kyoto Encyclopedia of Genes and Genomes (KEGG) analysis was performed using the web (https://www.kegg.jp/).

2.2.7. Quantitative real-time reverse transcription PCR (qPCR) analysis

The differentially expressed genes were further validated by qPCR (Wang et al., 2017). Primers were designed and provided from Wuhan servicebio technology CO., LTD. (Wuhan, China). The sequences were shown in Table S1. Revert Aid First Strand cDNA Synthesis Kit (Thermo) and Stepone plus fluorescence quantitative PCR instrument (ABI) were used to analyze the target genes expression level. Gapdh was used as internal control. The expression level of target genes was calculated by the following formula:

$$\text{Expression level} = 2^{-\Delta\Delta Ct}$$

$$\Delta\Delta Ct = A - B$$

A= Ct (target gene, pending test sample)
− CT (reference gene, pending test sample)

B= Ct (target gene, control sample)
− CT (reference gene, control sample)

2.2.8. Statistical analysis

All indexes were performed and analyzed in triplicates. Normally distributed variables were analyzed by one-way ANOVA followed by multiple comparisons post hoc significance test. Generalize linear logistic regression model was used to analyze the transcriptome data. SPSS 20 software (IBM, Chicago, USA) was employed for statistical analysis and a $p < 0.05$ was regarded as statistically significant.

3. Results and discussion

3.1. LC-TOF-MS/MS identification of RRE

The RRE compounds were identified based on the MS and MS/MS data of each peak. According to LC-TOF-MS/MS results (Table 1), there were 15 kinds of anthocyanins in RRE and their total relative abundance was add up to 60.08%. These compounds were as follows: cyanidin-3-O-di-hexoside (34.62%), cyanidin-3-O-glucoside (24.96%), cyaniding-3-O-rutinose (24.41%), cyanidin–glucosyl-rutinoside (7.93%), delphinidin-3-O-galactoside (2.55%), peonidin-3-O-arabinoside (2.36%), delphinidin 3-O-glucoside (0.945%), delphinidin-3-O-arabinoside (0.61%), peonidin-3-O-rutinose (0.44%), peonidin-3-O-galactoside (0.36%), cyanidin-3-O-galactoside (0.31%), delphinidin-3-O-(6″caffeoyl)-glucose (0.15%), cyanidin-3-O-arabinoside (0.11%), delphinidin-3-O-(6″methyl) glucoside (0.03%). Other polyphenols such as procyanindin B2 and (−)-epicatechin were identified with total abundance of 17.93%. In addition, there were a small amount of acid substances in RRE such as ellagic acid (7.16%), citric acid (4.07%), p-coumaric acid (1.92%) and asiatic acid (0.15%).

Anthocyanins showed good stability under acidic conditions and the evidence indicated that the anthocyanins were mainly metabolized into phenolic acids in the intestines, which were further absorbed and utilized by intestinal cell (Hidalgo et al., 2012; Letizia Bresciani et al., 2019). However, the type of metabolites were related to the anthocyanins composition. Mulberry anthocyanins were mainly converted to cryptochlorogenic acid, chlorogenic acid, caffeic acid, and ferulic acid (Cheng et al., 2016). By co-culturing elderberry anthocyanin in human intestinal bacteria, it was discovered that anthocyanins were eventually metabolized into gallic acid, syringic acid and p-coumaric acid (Letizia Bresciani et al., 2019). The metabolites of cyanidin 3-glucoside *in vivo* were mainly gallic acid, vanillic acid, caffeic acid and p-coumaric acids (Chen et al., 2017), which could ameliorate metabolic syndrome

Table 1
LC-Q/TOF-MS analysis of RRE composition.

Formula	Name	MS	MS/MS	Mass error (ppm)	Relative abundance (‰)
$C_{27}H_{31}O_{16}$	Cyanidin-3-O-di-hexoside	611.1602	287.0648(Cyanidin)	−0.7	207.98
$C_{21}H_{21}O_{11}$	Cyanidin-3-O-glucoside	449.1070	287.0629(Cyanidin)	−2.0	149.97
$C_{27}H_{31}O_{15}$	Cyanidin 3-O-rutinose	595.1653	449.1072(Cyanidin-3-O-glucoside),287.0611(Cyanidin)	3.2	146.84
$C_{30}H_{26}O_{12}$	Procyanindin B2	579.1489	127.0388, 163.0392, 271.0601	1.3	114.38
$C_{14}H_6O_8$	Ellagic acid	300.9990	300.9992, 283.9963, 229.0143	0.1	71.55
$C_{15}H_{14}O_6$	(−)-epicatechin	289.0718	123.0453, 125.0244, 203.0714	0.3	64.95
$C_{33}H_{41}O_{20}$	Cyanidin-glucosyl-rutinoside	757.2163	287.0608(Cyanidin)	1.3	47.63
$C_6H_8O_7$	Citric Acid	191.0198	87.0088, 111.0087, 67.0188	0.3	40.72
$C_9H_8O_4$	Caffeic acid	179.0349	135.0452, 134.0375	0.2	33.14
$C_9H_8O_3$	p-Coumaric acid	163.0400	119.0505, 93.0348, 117.0346	0.4	19.19
$C_{21}H_{20}O_{12}$	Hyperoside	463.0879	300.0275, 301.0352, 271.0246	0.6	17.77
$C_{21}H_{21}O_{12}$	Delphinidin 3-O-galactoside	465.1031	303.0493 (Delphinidin)	3.4	15.29
$C_{21}H_{21}O_{10}$	Peonidin-3-O-arabinoside	433.0733	301.0353(Peonidin)	1.1	14.15
$C_{21}H_{20}O_{10}$	Genistin	433.1126	271.059	2.7	12.76
$C_{26}H_{32}O_{11}$	Rosin monomethyl ether-D-glucoside	519.1876	357.1338, 151.0398, 136.0161	0.8	7.60
$C_{21}H_{20}O_{11}$	Luteoloside	449.1708	287.1205, 449.1773	2.1	6.13
$C_{21}H_{21}O_{12}$	Delphinidin 3-O-glucoside	465.1031	303.0493 (Delphinidin)	1.5	5.66
$C_{36}H_{58}O_{10}$	pedunculoside	668.4366	453.3364, 201.1638, 471.3467, 668.4367	1.2	3.96
$C_{20}H_{19}O_{11}$	Delphinidin-3-O-arabinoside	435.0925	303.0494 (Delphinidin)	0.8	3.69
$C_{20}H_{18}ClNO_4$	Berberine	336.1232	336.1234, 292.0972, 278.0817	0.4	2.86
$C_{15}H_{10}O_7$	Quercetin dihydrate	303.0499	303.0499, 229.0495, 153.0187	0.2	2.69
$C_{28}H_{33}O_{15}$	Peonidin 3-O-rutinose	609.1818	301.0716(Peonidin)	0.6	2.67
$C_{22}H_{23}O_{11}$	Peonidin-3-O-galactoside	463.1723	301.0704(Peonidin)	1.1	2.14
$C_{21}H_{21}O_{11}$	Cyanidin-3-O-galactoside	449.1070	287.0629(Cyanidin)	0.7	1.89
$C_{30}H_{48}O_5$	Asiatic acid	487.3425	487.3421, 169.3316	0.8	1.52
$C_{28}H_{33}O_{16}$	Peonidin 3-O-di hexoside	625.1407	301.0351(Peonidin)	0.1	1.04
$C_{30}H_{27}O_{15}$	Delphinidin-3-O-(6caffeoyl)-glucose	627.1556	303.0495 (Delphinidin)	3.4	0.95
$C_{20}H_{19}O_{10}$	Cyanidin-3-O-arabinoside	419.0969	287.0557(Cyanidin)	−0.2	0.65
$C_{22}H_{23}O_{12}$	Delphinidin-3-O-(6 methyl) glucoside	479.0822	303.0493 (Delphinidin)	1.3	0.21

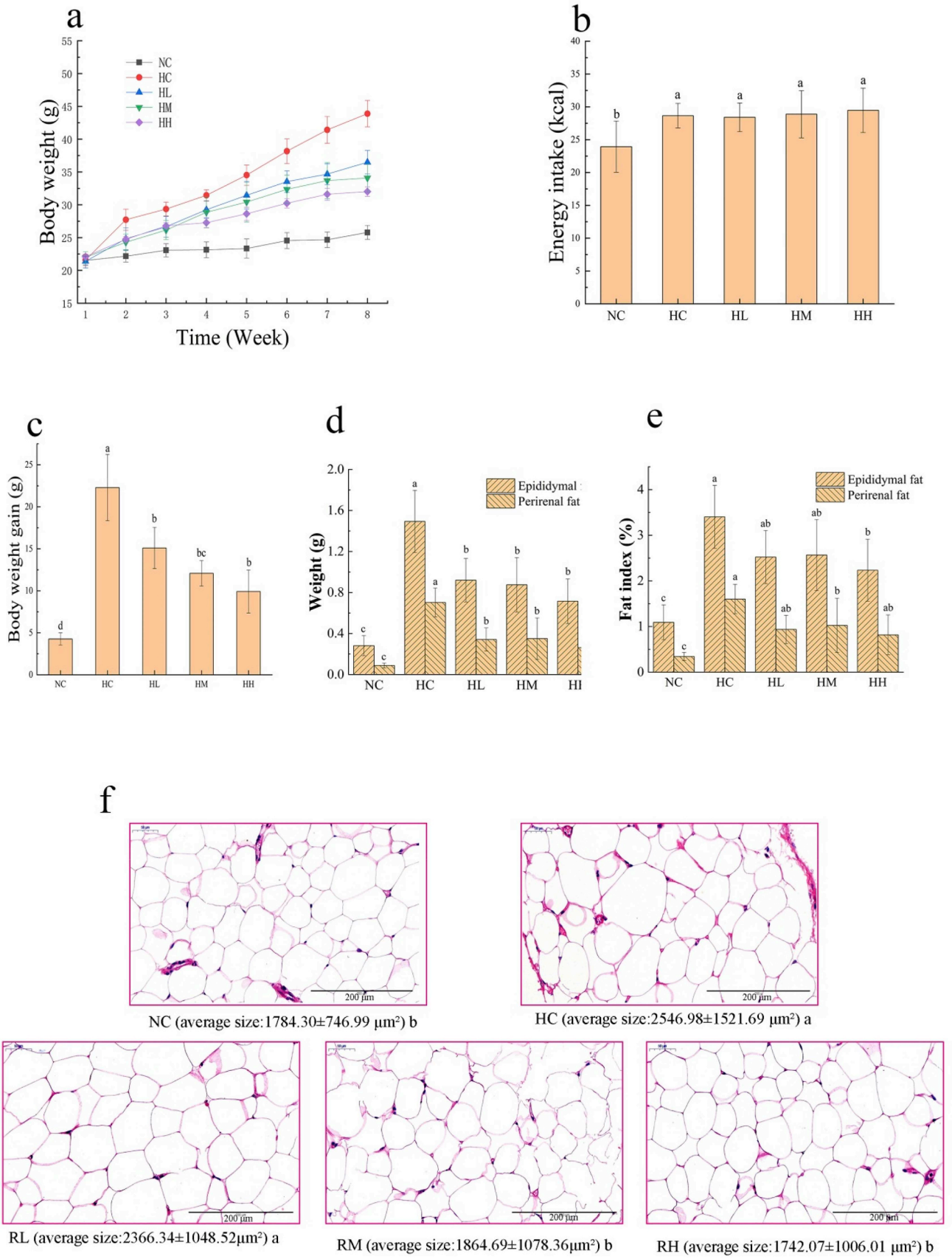

Fig. 1. Effects of RRE on body weight change (a), energy intake (b), body weight gain (c), epididymal and perirenal adipose tissue (d), epididymal and perirenal adipose tissue weight index (e), epididymal adipocytes size (f). Different alphabets on the data mean significant differences compared with other groups ($p < 0.05$).

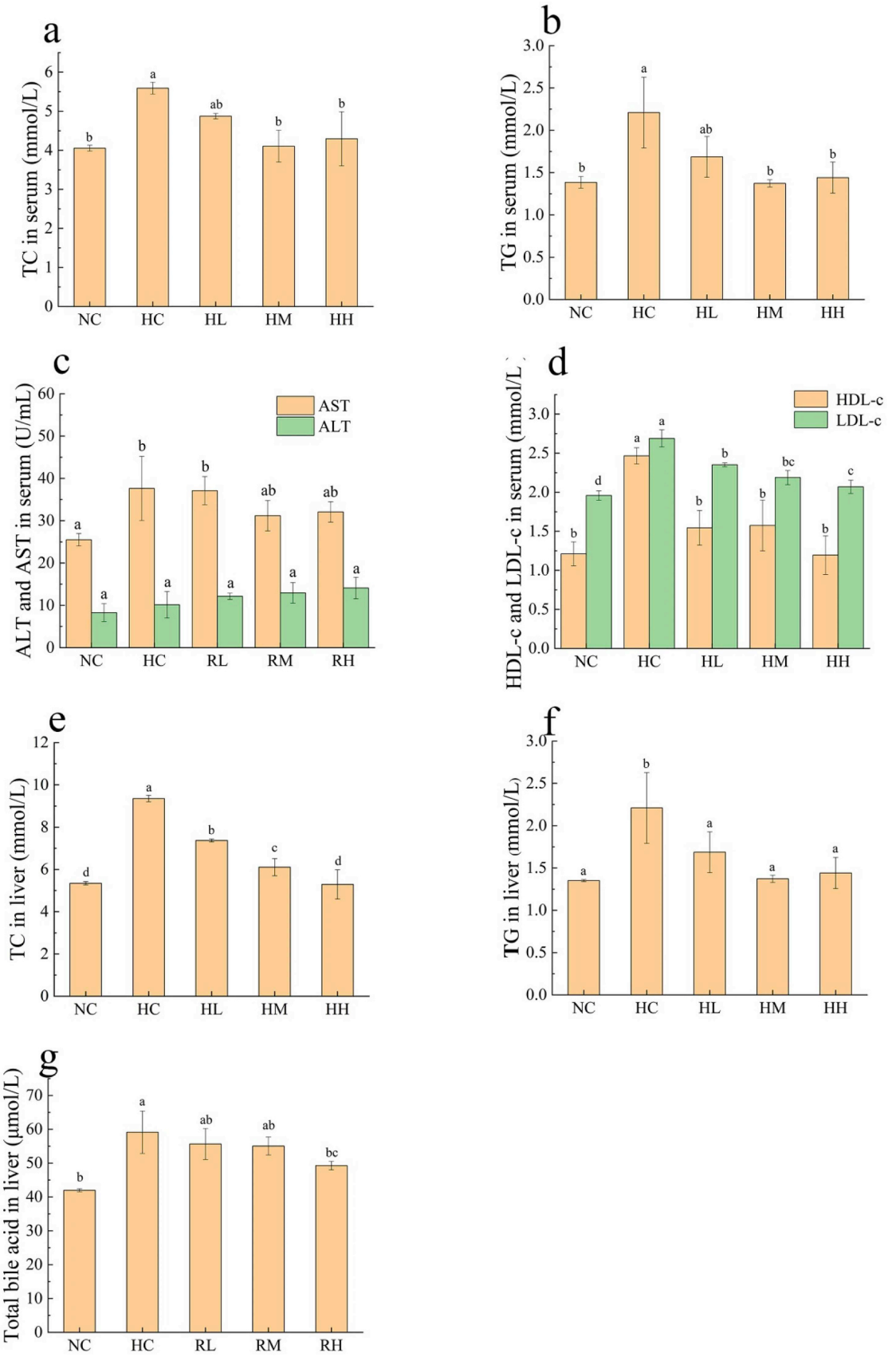

Fig. 2. Effects of RRE on CAT in serum (a) and liver (b), SOD in serum (c) and liver (d), MDA in serum (e) and liver (f), GSH-PX in serum (g) and liver (h). Different alphabets on the data mean significant differences compared with other groups ($p < 0.05$). Different alphabets on the data mean significant differences compared with other groups.

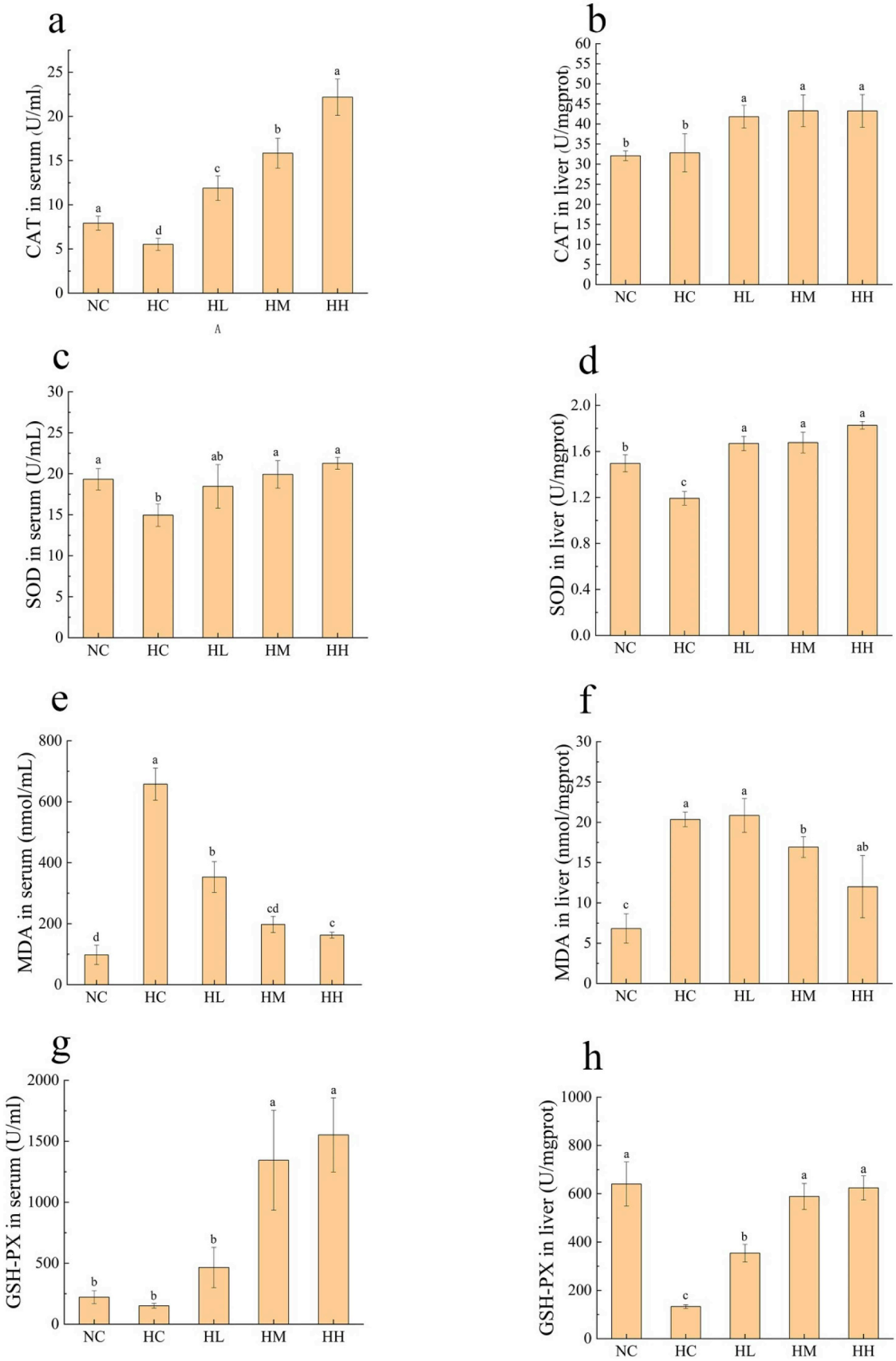

Fig. 3. Effects of RRE intake on TC level in serum (a), TG level in serum(b), ALT and AST in serum (c), HDL-c and LDL-c in serum (d), TC level in liver (e), TG level in liver (f), total bile acid level in liver (g). Different alphabets on the data mean significant differences compared with other groups ($p < 0.05$).

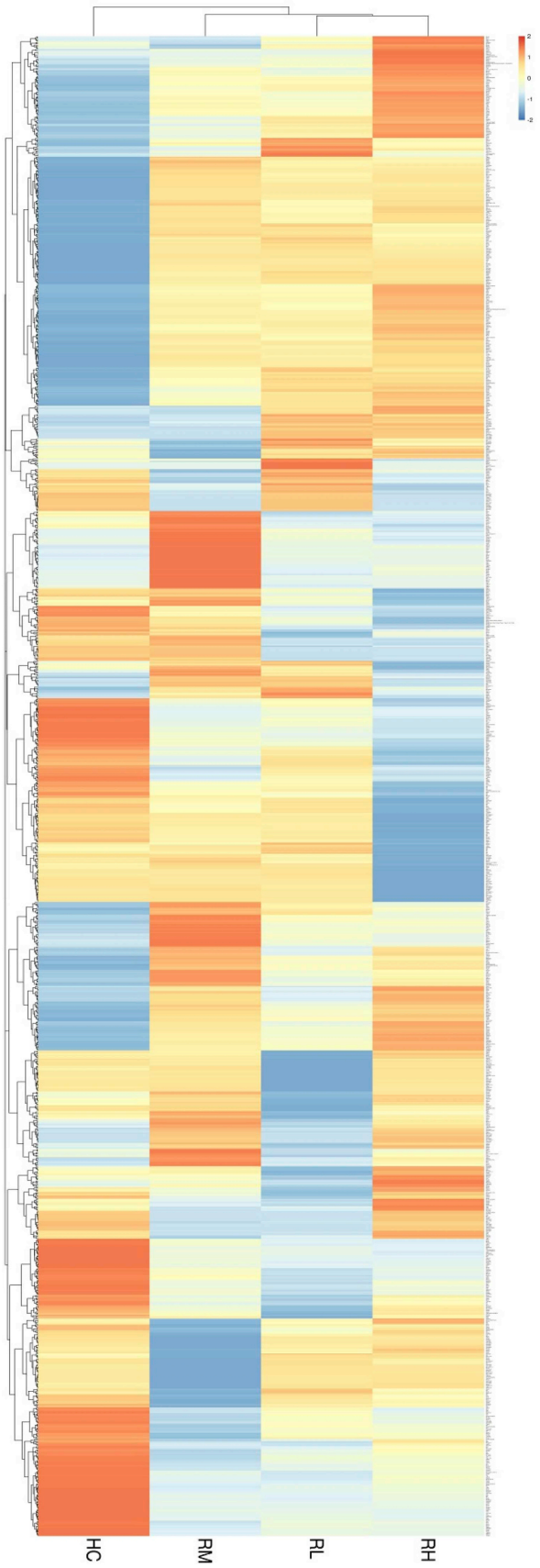

Fig. 4. Heat map of the differentially expressed genes ($p < 0.05$). Y-axis shows the list of genes and X-axis shows control and samples. Red fields show up-regulation of genes and green fields show down-regulation of genes. (For interpretation of the references to colour in this figure legend, the reader is referred to the Web version of this article.)

induced by high fat diet in rats (Guo et al., 2017). Vanillic acid treatment showed protective effects of hyperinsulinemia, hyperglycemia and hyperlipidemia in HFD rats (Chang et al., 2015). It was reported that ferulic acid could lower the lipid levels in diabetic rats and prevent complications (Balasubashini et al., 2003). Then it could be speculated that RRE compounds might have a positive effect on lipid metabolism due to the phenolic acids from anthocyanin metabolism.

3.2. Body weight and adipose tissue change in animal experiment

The body weight of the HFD control mice (HC) increased by 70.16% after 8 weeks compared to NC group. After RRE treatment for 8 weeks, body weight, epididymal and perirenal adipose tissue weight in HH group significantly reduced by 25.58%, 52.12% and 62.80% compared to HC group (Fig. 1a, c, d, e). Roopchand et al. (2013) demonstrated that blueberry polyphenol-enriched soybean flour showed anti-obesity capacity. However, there was no significant food energy intake difference between HC group and RRE treatment groups (Fig. 1b). As shown in Fig. 1f, average size of adipocytes in HC group was up to 2546.68 μm^2. Meanwhile, Average size of adipocytes in NC, RL, RM and RH were 1784.30, 2366.34, 1864.69 and 1742.07 μm^2, respectively. Since the fat accumulation was associated with the expansion of adipocyte resulting in hyperplasia and hypertrophy (Kalamaki et al., 2003; Lee et al., 2016), the reduction of adipocytes size (Fig. 1f) in RRE treatment groups further suggested that RRE could attenuate fat accumulation induced by HFD.

3.3. Antioxidant status in the serum and liver

HFD could led to an increase in free radical generation *in vivo* because of lipid peroxidation (Mattson, 2009). Superoxide dismutase (SOD), catalase (CAT) and glutathione peroxidase (GSH-PX) could scavenge reactive oxygen species and the other products of lipid peroxidation resulting in ameliorating oxidative stress (Chen et al., 2010). The SOD, CAT and GSH-PX level decreased in HC group compared with that of NC group (Fig. 2). Meanwhile, there was no significant difference between NC and RRE groups in antioxidant capacity suggesting that RRE administration could protect cells from oxidative damage. RRE treatment decreased the lipid peroxide malondialdehyde (MDA) indicating that RRE could enhance the antioxidant enzyme activity *in vivo*. The enhanced antioxidant activity demonstrated RRE intake could ameliorate oxidative stress induced by HFD.

3.4. Triglyceride and cholesterol level

As shown in Fig. 3, TC, TG, LDL-C, HDL-C levels of HC group were significant higher than those of NC group, which were consistent with the trends of body weight and fat accumulation. RRE supplementation strongly reduced TC, TG, LDL-C, HDL-C levels and the influence degree was presented as dose-dependent. Meanwhile, bile acid, which was the main cholesterol metabolite in liver, decreased by 5.88%, 6.92% and 16.67% in RL, RM and RH groups, respectively, compared to HC group. Lowering blood lipids such as TG and TC, was the most important strategy for preventing hyperlipidemia (Guo et al., 2011). However, the molecular mechanism of RRE hypolipidemic effect remains unclear. In addition, no significant ALT difference was observed between HC and RRE treatment groups. Compared to HC groups, the decrease of AST levels in RRE groups indicated that RRE intake would not lead to liver damages. The unusual weights, chemical compounds and enzymes levels were all correlated with lipid metabolism disorder. RRE intake might ameliorated these symptoms by regulating lipid metabolism.

3.5. Distribution of regulated genes in liver

Liver is the main organ for lipid metabolism (Pan et al., 2017). According to transcriptome analysis, many gene expressions declared

significant differences caused by RRE intake. The differentially expressed genes were drawn as heat maps (Fig. 4). Compared with HC group, 263 gene expressions were down-regulated and 375 gene expressions were up-regulated in HL group. Higher dose of RRE intake resulted in a greater number of differentially expressed genes (HM: 369 turn up and 386 turn down, HH: 476 turn up and 511 turn down).

After validated by qPCR, Pparα gene was up-regulated in all RRE treated groups. PPARs were known as regulator for fatty acid oxidation and lipid metabolism. Up-regulation of PPAR expression would lead to stimulation of lipolysis and inhibition of fatty acid synthesis in the liver (Den et al., 2015). It was reported that major urinary proteins (Mups) could regulate lipid metabolism through the hepatic lipogenic paracrine and autocrine (Wang et al., 2017). Many Mups genes expression were down-regulated after RRE administration. In addition, many genes related to oxidative stress, such as Heme oxygenase (Hmox1) and Glyceraldehyde-3-phosphate dehydrogenase (Gapdh), showed significant differences after RRE treatment (Si et al., 2017). Gapdh was a key enzyme in the glycolytic pathway that could catalyze the conversion of glyceraldehyde-3-phosphate to 1,3-glyceraldehyde diphosphate, while NAD+ was used as a hydrogen-receiving body to generate NADH (Mazurek et al., 2011). Hmox (heme oxygenase) was important for the degradation of heme into equimolar amounts of biliverdin, carbon monoxide, and iron. The gene encoding Hmox1 could produce an oxidative cellular stress involving the generation of reactive oxygen species (ROS) (Mazurek et al., 2011).

Compared with HC group, the differentially expressed genes were enriched in 648, 741 and 747 GO terms in HL, HM and HH groups, respectively. For biological process, many GO terms related to lipid metabolism showed significant differences (Table 2). In cholesterol metabolic process (GO: 0008203), Vldlr, Prkaa2, Gtf2h5 and Cdca7 genes were up-regulated, and Nfil3, Nrep and Ldlrap1 were down-regulated. In lipid storage (GO: 0019915), seven gene expressions (Mup5, Mup13, Mup11, Mup9, Tuft1, Lasp1 and Ern1) were down-regulated and two gene expressions (Crp, Nr0b2) were up-regulated. In cellular triglyceride homeostasis (GO: 0035356) term, total two genes expression were up-regulated, indicating that the regulation of intracellular triglycerides was accelerated. Furthermore, some enriched GO terms related to anti-oxidation were presented in Table 2 such as oxidation-reduction process (GO: 0055114), positive regulation of fatty acid beta-oxidation (GO: 0032000) and cellular response to hydrogen peroxide (GO: 0070301). Those GO terms demonstrated that RRE intake would suppress oxidative stress caused by high-fat diet. According to GO analysis, molecular functions were related to protein binding, DNA binding, transcription factor activity, sequence-specific DNA binding and oxidoreductase activity, etc. As shown in Table 2, the cellular components involved encompassed the nucleus, endoplasmic reticulum membrane, intracellular membrane-bounded organelle, microtubule cytoskeleton and organelle membrane, etc.

3.6. KEGG pathway analysis

Through KEGG pathway analysis, it was found that some differentially expressed genes were enriched in bile secretion, PPAR signaling pathway, fatty acid elongation, fatty acid metabolism and adipocytokine signaling pathway, which were related to hyperlipidemia (Table 3). The different expressions of Cyp7a1, Hmgcr, Ldlr, Slc10a2 and Slco1a4 contributed to the difference in bile secretion pathway in RRE treatment groups. In PPAR signaling pathway, Acsl3, Acsl4, Cyp4a14, Cyp4a32, Cyp7a1, Plin5 and Pparα were all differentially regulated in RRE treatment groups.

PPAR was a transcription factor that could regulate genes expression to modify tissue lipolysis and blood lipoprotein metabolism. PPAR agonist drugs could decrease plasma TG and TC level such as thiazolidinediones and fibrates (Seymour et al., 2008). As shown in Fig. 5, in order to investigate action of RRE on lipid metabolism, the expression levels of PPARα and its responsive genes were marked in KEGG

Table 2
GO terms related to hyperlipidemia in RRA treatment groups.

GO function	GO ID	GO term	HL (p)	HM (p)	HH (p)
Biological process	GO:0008202	steroid metabolic process	2.37E-05	3.49E-11	3.41E-07
	GO:0006694	steroid biosynthetic process	2.82E-02	8.87E-08	3.76E-05
	GO:0043401	steroid hormone mediated signaling pathway	1.90E-03	1.93E-02	4.56E-03
	GO:0019915	lipid storage	3.82E-02	1.76E-03	2.38E-02
	GO:0006629	lipid metabolic process	1.22E-04	1.39E-07	5.11E-04
	GO:0042632	cholesterol homeostasis	9.94E-03	1.01E-05	1.87E-02
	GO:0008203	cholesterol metabolic process	7.34E-03	4.05E-07	9.38E-07
	GO:0006707	cholesterol catabolic process	2.25E-02	3.15E-02	4.68E-02
	GO:2000188	regulation of cholesterol homeostasis	2.25E-02	3.15E-02	4.22E-03
	GO:0071222	cellular response to lipopolysaccharide	5.38E-06	5.56E-07	1.41E-03
	GO:0055114	oxidation-reduction process	1.98E-02	1.76E-05	3.52E-02
	GO:0032000	positive regulation of fatty acid beta-oxidation	2.25E-02	3.15E-02	4.22E-03
	GO:0070301	cellular response to hydrogen peroxide	3.22E-02	5.18E-03	4.77E-02
	GO:0032000	positive regulation of fatty acid beta-oxidation	2.25E-02	3.15E-02	4.22E-03
	GO:0001676	long-chain fatty acid metabolic process	3.24E-03	6.17E-03	2.40E-04
	GO:0032000	positive regulation of fatty acid beta-oxidation	2.25E-02	3.15E-02	4.22E-03
Cellular component	GO:0005634	nucleus	5.15E-04	1.90E-03	6.49E-04
	GO:0005789	endoplasmic reticulum membrane	1.23E-04	3.84E-04	6.50E-04
	GO:0043231	intracellular membrane-bounded organelle	6.83E-03	1.92E-02	1.30E-02
	GO:0015630	microtubule cytoskeleton	1.42E-02	4.22E-02	1.56E-02
	GO:0031090	organelle membrane	5.01E-03	1.56E-05	1.41E-04
	GO:0005515	protein binding	8.68E-03	3.91E-03	1.03E-01
	GO:0003677	DNA binding	3.82E-02	9.18E-03	1.94E-03
	GO:0003700	transcription factor activity, sequence-specific DNA binding	9.54E-04	2.14E-05	1.94E-03
Molecular function	GO:0016491	oxidoreductase activity	1.02E-02	9.28E-06	3.54E-02
	GO:0031625	ubiquitin protein ligase binding	1.42E-05	5.79E-04	1.53E-02
	GO:0043565	sequence-specific DNA binding	4.79E-02	8.03E-03	5.13E-04
	GO:0008134	transcription factor binding	6.80E-04	6.11E-03	9.50E-07

HL: HFD-low does RRE group.
HM: HFD-middle does RRE group.
HH: HFD-high does RRE group.

Table 3
KEGG pathways related to hyperlipidemia in RRA treatment groups.

Group	pathway ID	pathway name	genes name	up-regluated genes number	Significant gene number	p
HL	ko04920	Adipocytokine signaling pathway	Acsl3, Acsl4, G6pc, Mapk8, Pparα, Prkaa2, Prkab2, Socs3, Tnfrsf1b	2	9	9.07E-04
	ko04976	Bile secretion	Atp1b2, Cyp7a1, Hmgcr, Ldlr, Nceh1, Nr0b2, Slc10a2, Slco1a4	4	8	3.70E-03
	ko03320	PPAR signaling pathway	Acsl3, Acsl4, Cyp4a14, Cyp4a32, Cyp7a1, Plin5, Pparα	3	7	2.29E-02
HM	ko04976	Bile secretion	Abcb1a, Abcb1b, Abcg5, Abcg8, Adcy1, Aqp8, Atp1a3, Atp1b2, Cyp7a1, Hmgcr, Kcnn2, Ldlr, Slc10a2, Slco1a4	8	14	1.38E-06
	ko03320	PPAR signaling pathway	Acsl3, Cpt1b, Cyp4a10, Cyp4a14, Cyp7a1, Fabp4, Lpl, Plin4, Plin5, Ppard, Scd1, Scd2, Slc27a1	10	13	2.68E-05
	ko00062	Fatty acid elongation	Acsl3, Cpt1b, Cyp4a10, Cyp4a14	3	4	2.48E-02
	ko04920	Adipocytokine signaling pathway	Acsl3, Cpt1b, G6pc, Mapk8, Prkaa2, Socs3, Tnfrsf1b	1	7	3.20E-02
HL	ko03320	PPAR signaling pathway	Acsl3, Acsl4, Cpt1a, Cyp4a14, Cyp4a32, Cyp7a1, Ehhadh, Fabp5, Plin4, Plin5, Pparα	6	11	1.12E-03
	ko04976	Bile secretion	Abcg5, Abcg8, Adcy1, Cyp7a1, Hmgcr, Ldlr, Nr0b2, Slc10a2, Slco1a4	4	9	5.83E-03
	ko00071	Fatty acid degradation	Acsl3, Acsl4, Cpt1a, Cyp4a14, Cyp4a32, Ehhadh	3	6	2.14E-02
	ko04920	Adipocytokine signaling pathway	Acsl3, Acsl4, Cpt1a, G6pc, Pparα, Slc2a4, Socs3, Tnfrsf1b	3	8	1.80E-02
	ko01212	Fatty acid metabolism	Acsl3, Acsl4, Cpt1a, Ehhadh, Elovl6, Hacd4	2	6	3.67E-02

HL: HFD-low does RRE group.
HM: HFD-middle does RRE group.
HH: HFD-high does RRE group.

pathway maps. PPARα expression level increased to 184%, 203% and 218% compared to that of HC group. It was obvious that RRE was regarded as a PPARα activator, and its target genes in lipid metabolism were significantly regulated in the liver following RRE administration.

Cholesterol homeostasis was related to cholesterol biosynthesis and the conversion of cholesterol to bile acids (Roopchand et al., 2013). Hydroxymethylglutaryl coenzyme A reductase (HMGCR) and cholesterol 7α-hydroxylase (CYP7A1) were the rate-limiting enzyme in the synthesis of cholesterol and the conversion of cholesterol to bile acid, respectively (Matsui et al., 2013). Cholesterol homeostasis was regulated by CYP7A1 and HMGCR. As shown in Fig. 5, HMGCR gene expression reduced to 12% in RRE treatment group compared to that of HC group. The reduction of HMGCR gene expression inhibited the conversion of HMG-CoA to mevalonate resulting in lower TC levels (Si et al., 2017). Down-regulated expression of Hmgcr gene could reduce cholesterol synthesis rate in RRE treatment groups (Fig. 5). LDL was the lipoprotein particle that carried cholesterol into peripheral tissue cells. Moreover, Ldlr gene receptor was also down-regulated by RRE intake, which would lead to the inhibition of cholesterol absorption. The reduction of cholesterol absorption would further promote the excretion of cholesterol resulting in the decrease of cholesterol level.

As shown in Fig. 5, Pnpla2 gene related to triacylglycerol lipase increased to 210%, 225% and 267% in HL, HM and HH groups, respectively, compared to HC group. It was obvious that more active triacylglycerol lipase could accelerate the conversion from TG to fatty acid (Kuok Teong et al., 2011). Moreover, more active triacylglycerol lipase could also accelerate the conversion from 1,2-Diacylglycerol to glyceride and fatty acid.

Long-chain acyl-CoA synthetase (ACSL) catalyzed conversion of fatty acids to fatty acyl-CoA is the first step in fatty acid metabolism (Jia et al., 2007). Acsl3 gene (encoding ACSL) were down-regulated in RRE treated groups, which would reduce fatty acid utilization and fat accumulation and be well associated with body and liver weight gain results. According to adipocyte signal pathway, fatty acyl CoA could be further transported to the mitochondria for beta oxidation to produce energy and acetyl-CoA. A large number of reactive oxygen species was accompanied with the beta oxidation which could reduce antioxidant enzyme activity *in vivo*.

As confirmed by the previous studies, tart cherry anthocyanins intake regulated the activity of PPARs (Seymour et al., 2008), and gallic acid treatment could significantly increase PPAR expression in the adipose tissue of diabetic rat (Gandhi et al., 2014). Meanwhile, ellagic acid, p-coumaric acid and ferulic acid intake would activate PPAR (Nankar and Doble, 2015; Ramaa et al., 2016). In a short, up-regulation of PPARα regulated the transcription of PPARα target genes involved in lipid metabolism, such as Cyp7a1, Hmgcr, Ldlr, Acsl3, Pnpla2 and Pin5, thus leading to the decrease of triglyceride and cholesterol levels in hepatocytes (Jia et al., 2011; Rakhshandehroo et al., 2010). It has been confirmed that Ldlr, Hmgcr and Cyp7a1 genes was regulated by elderberry extract resulting in a reduction of hepatic cholesterol levels (Farrell et al., 2015). In addition, hepatic TG storage would be reduced by PPARα activation via activating Pnpla2 gene resulting in stimulating the TG hydrolysis pathway (Rakhshandehroo et al., 2010).

4. Conclusion

This study demonstrated that RRE could efficiently attenuate lipid metabolism disorder in the hyperlipidemia mice induced by HFD. RRE intake significantly ($p < 0.05$) decreased TC and TG level together with improving antioxidant status in hyperlipidemia mice. Enhanced antioxidant enzyme activity might protect cells from oxidative damage. RRE was regarded as an agonist, regulating lipid metabolism related genes. A RRE dietary intervention might be a viable supplementary prevention of hyperlipidemia.

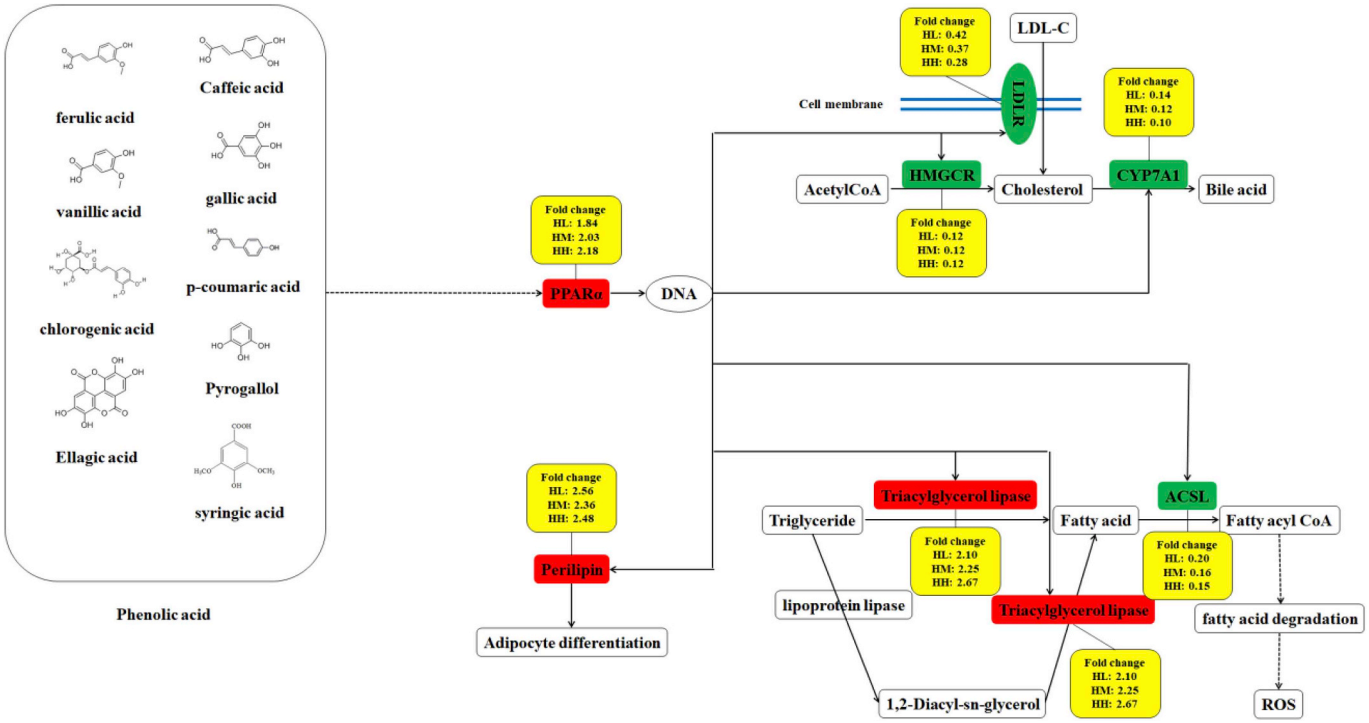

Fig. 5. Hypolipidemic molecular mechanism of RRE intake. Red filling represents the acting site of the up-regulating genes ($p < 0.05$). Blue filling represents the acting site of the down-regulating genes ($p < 0.05$). Yellow filling represents the genes expression fold change. HL: HFD-low does RRE group. HM: HFD-middle does RRE group. HH: HFD-high does RRE group. (For interpretation of the references to colour in this figure legend, the reader is referred to the Web version of this article.)

Declaration of Competing Interest

The authors declare that they have no known competing financial interests or personal relationships that could have appeared to influence the work reported in this paper.

Acknowledgment

We thank AB Sciex Pte. Ltd. and Hangzhou Lianchuan Biotechnology Co., Ltd. for laboratory technical supports with LC-TOF-MS/MS identification and transcriptome analysis work.

Transparency document

Transparency document related to this article can be found online at https://doi.org/10.1016/j.fct.2019.110796.

Appendix A. Supplementary data

Supplementary data to this article can be found online at https://doi.org/10.1016/j.fct.2019.110796.

Funding

This study was funded by the Natural Science Foundation of China (No. 31771974, 31701524), the Anhui Provincial Natural Science Foundation, China (No. 1708085MC70), the Fundamental Research Funds for the Central Universities, China (No. JZ2018HGTB0245, No. JZ2019YYPY0295) and Chengdu Technological Innovation Research and Development Project, China (2019-YF05-00965-SN).

References

Abdel-Aal, E.S.M., Hucl, P., Rabalski, I., 2018. Compositional and antioxidant properties of anthocyanin-rich products prepared from purple wheat. Food Chem. 254, 13–19.

Balasubashini, M.S., Rukkumani, R., Menon, V.P., 2003. Protective effects of ferulic acid on hyperlipidemic diabetic rats. Acta Diabetol. 40, 118–122.

Bell, D.R., Kristen, G., 2006. Direct vasoactive and vasoprotective properties of anthocyanin-rich extracts. J. Appl. Physiol. 100, 1164–1170.

Bibi, S., Du, M., Zhu, M.J., 2018. Dietary red raspberry reduces colorectal inflammation and carcinogenic risk in mice with dextran sulfate sodium-induced colitis. J. Nutr. 5, 667–674.

Chang, W.C., James, W., Chen-Wen, C., Po-Ling, K., Hsu-Min, C., Yuh-Tai, W., Szu-Chuan, S., 2015. Protective effect of vanillic acid against hyperinsulinemia, hyperglycemia and hyperlipidemia via alleviating hepatic insulin resistance and inflammation in high-fat diet (HFD)-Fed rats. Nutrients 7, 9946–9959.

Chen, H., Liu, L.J., Zhu, J.J., Xu, B., Li, R., 2010. Effect of soybean oligosaccharides on blood lipid, glucose levels and antioxidant enzymes activity in high fat rats. Food Chem. 119, 1633–1636.

Chen, Y., Li, Q., Zhao, T., Zhang, Z., Mao, G., Feng, W., Wu, X., Yang, L., 2017. Biotransformation and metabolism of three mulberry anthocyanin monomers by rat gut microflora. Food Chem. 237, 887–894.

Cheng, J.R., Liu, X.M., Chen, Z.Y., Zhang, Y.S., Zhang, Y.H., 2016. Mulberry anthocyanin biotransformation by intestinal probiotics. Food Chem. 213, 721–727.

Den, G.B., Bleeker, A., Gerding, A., Van, K.E., Havinga, R., Van, T.D., Oosterveer, M.H., Jonker, J.W., Groen, A.K., Reijngoud, D.J., 2015. Short-chain fatty acids protect against high-fat diet-induced obesity via a PPARγ-dependent switch from lipogenesis to fat oxidation. Diabetes 64, 2398–2408.

Durgo, K., Belščakcvitanović, A., Stančić, A., Franekić, J., Komes, D., 2012. The bioactive potential of red raspberry (Rubus idaeus L.) leaves in exhibiting cytotoxic and cytoprotective activity on human laryngeal carcinoma and colon adenocarcinoma. J. Med. Food 15, 258–268.

Farrell, N., Norris, G., Sang, G.L., Chun, O.K., Blesso, C.N., 2015. Anthocyanin-rich black elderberry extract improves markers of HDL function and reduces aortic cholesterol in hyperlipidemic mice. Food & Function 6, 1278–1287.

Gandhi, G.R., Jothi, G., Antony, P.J., Balakrishna, K., Paulraj, M.G., Ignacimuthu, S., Stalin, A., Aldhabi, N.A., 2014. Gallic acid attenuates high-fat diet fed-streptozotocin-induced insulin resistance via partial agonism of PPARγ in experimental type 2 diabetic rats and enhances glucose uptake through translocation and activation of GLUT4 in PI3K/p-Akt signaling pathway. Eur. J. Pharmacol. 745, 201–216.

Guo, F., Huang, C., Liao, X., Wang, Y., He, Y., Feng, R., Li, Y., Sun, C., 2011. Beneficial effects of mangiferin on hyperlipidemia in high-fat-fed hamsters. Mol. Nutr. Food Res. 55, 1809–1818.

Guo, X., Wang, O., Wang, Y., Wang, K., Ji, B., Zhou, F., 2017. Phenolic acids alleviate high-fat and high-fructose diet-induced metabolic disorders in rats. J. Food Biochem. 41 e12419.

Hidalgo, M., Oruna-Concha, M.J., Kolida, S., Walton, G.E., Kallithraka, S., Spencer, J.P., De, P.-T.S., 2012. Metabolism of anthocyanins by human gut microflora and their influence on gut bacterial growth. J. Agric. Food Chem. 60, 3882–3890.

Jia, Y., Bhuiyan, M.J.H., Jun, H.J., Ji, H.L., Hoang, M.H., Lee, H.J., Kim, N., Lee, D.,

Hwang, K.Y., Bang, Y.H., 2011. Ursolic acid is a PPAR-α agonist that regulates hepatic lipid metabolism. Bioorg. Med. Chem. Lett 21, 5876–5880.
Jia, Z., Moulson, C.L., Pei, Z., Miner, J.H., Watkins, P.A., 2007. FATP4 is the principal very long-chain fatty acyl-CoA synthetase in skin fibroblasts. J. Biol. Chem. 21, A607–A608.
Johnston, T.P., Korolenko, T.A., Sahebkar, A., 2017. The P-407-Induced mouse model of dose-controlled hyperlipidemia and atherosclerosis: twenty-five years later. J. Cardiovasc. Pharmacol. 70, 339–349.
Joseph, S.V., Edirisinghe, I., Burton-Freeman, B.M., 2016. Fruit polyphenols: a review of anti-inflammatory effects in humans. Crit. Rev. Food Technol. 56, 419–444.
Kalamaki, M.S., Powell, A.L., Struijs, K., Labavitch, J.M., Reid, D.S., Bennett, A.B., 2003. Transgenic overexpression of expansin influences particle size distribution and improves viscosity of tomato juice and paste. J. Agric. Food Chem. 51, 7465–7471.
Kuok Teong, O., Mashek, M.T., So Young, B., Greenberg, A.S., Mashek, D.G., 2011. Adipose triglyceride lipase is a major hepatic lipase that regulates triacylglycerol turnover and fatty acid signaling and partitioning. Hepatology 53, 116–126.
Lee, H.S., Lim, W.C., Lee, S.J., Lee, S.H., Lee, J.H., Cho, H.Y., 2016. Antiobesity effect of garlic extract fermented by lactobacillus plantarum BL2 in diet-induced obese mice. J. Med. Food 19, 823–829.
Letizia Bresciani, Angelino, Donato, Vivas, Eugenio I., García-Viguera, Cristina, Daniele Del Rio, Rey, Federico E., 2019. Differential catabolism of an anthocyanin-rich elderberry extract by three gut microbiota bacterial species. J. Agric. Food Chem. 45, 115–125.
Lin, Kun, J., Shiau, L., Yn, S., 2010. Mechanisms of hypolipidemic and anti-obesity effects of tea and tea polyphenols. Mol. Nutr. Food Res. 50, 211–217.
Matsui, S., Yamane, T., Takita, T., Oishi, Y., Kobayashi-Hattori, K., 2013. The hypocholesterolemic activity of Momordica charantia fruit is mediated by the altered cholesterol- and bile acid–regulating gene expression in rat liver. Nutr. Res. 33, 580–585.
Mattson, M.P., 2009. Roles of the lipid peroxidation product 4-hydroxynonenal in obesity, the metabolic syndrome, and associated vascular and neurodegenerative disorders. Exp. Gerontol. 44, 625–633.
Mazurek, B., Amarjargal, N., Haupt, H., Fuchs, J., Olze, H., Machulik, A., Gross, J., 2011. Expression of genes implicated in oxidative stress in the cochlea of newborn rats. Hear. Res. 277, 54–60.
Nankar, R.P., Doble, M., 2015. Ellagic acid potentiates insulin sensitising activity of pioglitazone in L6 myotubes. Journal of Functional Foods 15, 1–10.
Noratto, G.D., Chew, B.P., Atienza, L.M., 2017. Red raspberry (Rubus idaeus L.) intake decreases oxidative stress in obese diabetic (db/db) mice. Food Chem. 227, 305–314.
Pan, M.H., Yang, G., Li, S., Li, M.Y., Tsai, M.L., Wu, J.C., Badmaev, V., Ho, C.T., Lai, C.S., 2017. Combination of citrus polymethoxyflavones, green tea polyphenols and Lychee extracts suppresses obesity and hepatic steatosis in high-fat diet induced obese mice. Mol. Nutr. Food Res. 61, 1601104–1601113.
Park, H.J., Cho, J.Y., Mi, K.K., Koh, P.O., Cho, K.W., Kim, C.H., Lee, K.S., Chung, B.Y., Kim, G.S., Choa, J.H., 2012. Anti-obesity effect of Schisandra chinensis in 3T3-L1 cells and high fat diet-induced obese rats. Food Chem. 134, 227–234.
Rakhshandehroo, M., Knoch, B., Müller, M., Kersten, S., 2010. Peroxisome proliferator-activated receptor alpha target genes. PPAR Res. 2010, 393–416.
Ramaa, C.S., Gota, V., Marulkar, K., Joshi, H., 2016. Hydroxy cinnamic acid derivatives as partial PPAR agonists: in silico studies, synthesis and biological characterization against chronic myeloid leukemia cell line (K562). Anti Cancer Agents Med. Chem. 17, 524–541.
Roopchand, D.E., Kuhn, P., Rojo, L.E., Lila, M.A., Raskin, I., 2013. Blueberry polyphenol-enriched soybean flour reduces hyperglycemia, body weight gain and serum cholesterol in mice. Pharmacol. Res. 68, 59–67.
Seymour, E., Singer, A., A. Urcuyo-Llanes, D., Kaufman, P., Bolling, S., 2008. Altered hyperlipidemia, hepatic steatosis, and hepatic peroxisome proliferator-activated receptors in rats with intake of tart cherry. J. Med. Food 11, 252–259.
Si, X., Strappe, P., Blanchard, C., Zhou, Z., 2017. Enhanced anti-obesity effects of complex of resistant starch and chitosan in high fat diet fed rats. Carbohydr. Polym. 157, 834–841.
Souza, V.R.d., Silva, T.L.T.d., Lima, L.C.d.O., Pio, R., Queiroz, F., 2014. Determination of the bioactive compounds, antioxidant activity and chemical composition of Brazilian blackberry, red raspberry, strawberry, blueberry and sweet cherry fruits. Food Chem. 156, 362–368.
Wang, B., Zhang, S., Wang, X., Yang, S., Jiang, Q., Xu, Y., Xia, W., 2017. Transcriptome analysis of the effects of chitosan on the hyperlipidemia and oxidative stress in high-fat diet fed mice. Int. J. Biol. Macromol. 102, 104–110.
Zhu, Z., Lin, Z., Jiang, H., Jiang, Y., Zhao, M., Liu, X., 2017. Hypolipidemic effect of Youcha in hyperlipidemia rats induced by high-fat diet. Food & Function 8, 1680–1687.